microbial biotechnology

Open Access

Minireview

Shifts in xylanases and the microbial community associated with xylan biodegradation during treatment with rumen fluid

Shuhei Takizawa,[1,2,†] Ryoki Asano,[3] Yasuhiro Fukuda,[1] Yasunori Baba,[4] Chika Tada[1,*] and Yutaka Nakai[3,]**

[1]*Laboratory of Sustainable Animal Environment, Graduate School of Agricultural Science, Tohoku University, Osaki, Japan.*

[2]*Japan Society for the Promotion of Science, Chiyoda-ku, Japan.*

[3]*Department of Agro-Food Science, Faculty of Agro-Food Science, Niigata Agro-Food University, Tainai, Japan.*

[4]*Research Institute for Bioresources and Biotechnology, Ishikawa Prefectural University, Nonoichi, Japan.*

Summary

Treatment with rumen fluid improves methane production from non-degradable lignocellulosic biomass during subsequent methane fermentation; however, the kinetics of xylanases during treatment with rumen fluid remain unclear. This study aimed to identify key xylanases contributing to xylan degradation and their individual activities during xylan treatment with bovine rumen microorganisms. Xylan was treated with bovine rumen fluid at 37°C for 48 h under anaerobic conditions. Total solids were degraded into volatile fatty acids and gases during the first 24 h. Zymography showed that xylanases of 24, 34, 85, 180, and 200 kDa were highly active during the first 24 h. Therefore, these xylanases are considered to be crucial for xylan degradation during treatment with rumen fluid. Metagenomic analysis revealed that the rumen microbial community's structure and metabolic function temporally shifted during xylan biodegradation. Although statistical analyses did not reveal significantly positive correlations between xylanase activities and known xylanolytic bacterial genera, they positively correlated with protozoal (e.g., *Entodinium*, *Diploplastron*, and *Eudiplodinium*) and fungal (e.g., *Neocallimastix*, *Orpinomyces*, and *Olpidium*) genera and unclassified bacteria. Our findings suggest that rumen protozoa, fungi, and unclassified bacteria are associated with key xylanase activities, accelerating xylan biodegradation into volatile fatty acids and gases, during treatment of lignocellulosic biomass with rumen fluid.

Introduction

The rumen is an evolved forestomach and is one of the four stomachs in ruminants, hosting a complex rumen microbial community consisting of 10^{10} bacterial cells, 10^4 fungal cells, and 10^6 protozoal cells per ml (Castillo-González *et al.*, 2014). Ruminants do not produce glycoside hydrolases to degrade ingested lignocellulosic feeds; therefore, they depend on their rumen microbial community to convert ingested lignocellulosic feeds into volatile fatty acids (VFAs) as an energy source. Rumen microbial communities enable ruminants to provide readily accessible animal products (i.e., dairy products, meat, and leather) from human-indigestible lignocellulose. The rumen microbial community produces various fibrolytic enzymes, such as endoglucanase (EC 3.2.1.4), exoglucanase (EC 3.2.1.91), beta-glucosidase (EC 3.2.1.21), xylanase (EC 3.2.1.8), beta-xylosidase (EC 3.2.1.37), alfa-amylase (EC 3.2.1.37), and lignin peroxidase (EC 1.11.1.14), for the efficient digestion of undegradable plant materials into fermentable oligo- and monosaccharides (Wang *et al.*, 2019). In general, *Fibrobacter* and *Ruminococcus* are considered the major fibrolytic

Received 9 March, 2021; revised 3 November, 2021; accepted 24 November, 2021.
For correspondence. *E-mail chika.tada.e1@tohoku.ac.jp; Tel. +81 229 84 7395; Fax +81 229 84 7391. **E-mail yutaka-nakai@nafu.ac.jp; Tel. +81 254 28 9855; Fax +81 254 28 9856.
[†]Present address: Institute of Livestock and Grassland Science, National Agriculture and Food Research Organization, Tsukuba, Ibaraki, Japan.
Microbial Biotechnology (2022) **15**(6), 1729–1743
doi:10.1111/1751-7915.13988
Funding information
This work was supported by JSPS KAKENHI (grant numbers JP17H01512, JP19J12745, and JP21H04749), JST Adaptable and Seamless Technology transfer Program through Target-driven R&D (A-STEP), the Miyagi Prefectural Government Recycling Promotion Division, and the Miyagi Organization for Industry Promotion.

bacteria, whereas anaerobic fungi secrete a wide variety of polysaccharide-degrading enzymes and their rhizoidal system can physically penetrate lignified tissue that is not degraded by other microorganisms (Guo *et al.*, 2020). The high fibrolytic activities of these rumen microorganisms have attracted attention recently for the bioproduction of saccharides, VFAs, methane gas, and other valuable products from lignocellulosic biomass (Liang *et al.*, 2020). Lignocellulosic biomass, such as agricultural residues, paper waste, and forest residues, is one of the most abundant organic resources. The global annual production of lignocellulosic biomass is estimated to be approximately 181.5×10^9 tons, and 4.6×10^9 tons of lignocellulosic biomass residues are derived from agricultural residues (Dahmen *et al.*, 2018). Lignocellulosic biomass is mainly composed of carbohydrate polymers, such as cellulose, hemicellulose, and lignin. These polymers form a strong structure that resists disintegration and hydrolysis during anaerobic digestion (Sawatdeenarunat *et al.*, 2015). To accelerate the hydrolysis of polymers in lignocellulosic biomass, we previously proposed pretreatment of the biomass with rumen fluid discharged from slaughterhouses (Baba *et al.*, 2013). This pretreatment has been shown to improve methane gas production from rice straw (Zhang *et al.*, 2016), paper sludge (Takizawa *et al.*, 2018), and rapeseed (Baba *et al.*, 2017, 2019) by 1.5–3.4 times. Furthermore, low sodium dodecyl sulfate concentrations improve the efficiency of pretreatment with rumen fluid, enhancing methane production from waste paper (Takizawa *et al.*, 2020a,b,c).

Knowledge of the fibrolytic enzymes of ruminal microorganisms is vital for improving the biodegradation efficiency of lignocellulosic biomass during treatment with rumen fluid. We previously reported endoglucanase activity and the responsible microorganisms (Takizawa *et al.*, 2020a,b,c); however, hemicellulase activity has not yet been clarified. Xylan is the main component of hemicellulose, and the hydrolysis of xylan polymers is one of the rate-limiting steps in anaerobic degradation of lignocellulosic biomass. This study focused on xylanase in the rumen microbial community because xylanase catalyzes the hydrolysis of beta-1,4-glycosidic linkages of xylan polymers, producing xylooligosaccharides and xyloses. Biochemical analyses of crude enzymes have revealed that isolated and/or cultivated ruminal bacteria, protozoa, and fungi produce various xylanases (Wereszka *et al.*, 2006; Novotná *et al.*, 2010; Nyonyo *et al.*, 2014). Recently, culture-independent approaches have played an important role in defining the rumen microbial community. Metatranscriptomic analysis has revealed that two-thirds of the transcripts annotated as putative hemicellulases were produced by members of the characterized genera *Ruminococcus*, *Fibrobacter*, and *Prevotella*, suggesting that these fibrolytic genera are predominant degraders of plant cell-wall polysaccharide in the bovine rumen (Dai *et al.*, 2015; Comtet-Marre *et al.*, 2017). However, these previous studies did not investigate individual xylanases in complex microbial ecosystems.

Additionally, the relationship between individual xylanase activities and the rumen microbial community during treatment with rumen fluid remains obscure. This study aimed to determine individual xylanase activities during treatment with rumen fluid and the rumen microorganisms associated with xylan degradation. We determined the chemical characteristics of xylan degradation, individual xylanase activities, and the rumen microbial community's structure and metabolic function during xylan treatment with bovine rumen fluid. Additionally, we compared the correlations between key xylanase activities and microbial abundances.

Results

Chemical characteristics of xylan degradation by the rumen microbiota

Xylan was degraded by a bovine rumen microbial community during treatment for 48 h (Fig. 1). The total solids (TS) concentration decreased from 6.7 to 5.1 g reactor^{-1} during 48 h, and 23.4% of the TS was degraded after the treatment (Fig. 1A). The TS degradation rate did not change during the first 24 h; however, it significantly decreased from 24 h to 48 h (Fig. 1B). With xylan degradation, xylan metabolic products increased during treatment. Reducing sugars decreased from 6.4 to 0.7 g l^{-1} during the first 24 h (Fig. 1C). The dominant VFA produced throughout treatment was acetic acid, followed by propionic acid and butyric acid (Fig. 1D). Additionally, lactic acid was detected after 24 h at a concentration comparable to that of butyric acid. The total VFA concentration significantly increased 3.2 times (from 74.4 to 236.6 mmol l^{-1}) during the first 24 h. The pH decreased from 7.3 to 4.6 during the first 24 h (Fig. 1E), which reflected the increase in the total VFA concentration. Alongside the increase in total VFAs, the volumes of carbon dioxide gas and methane gas increased 2.3 and 2.2 times, respectively, between 6 h and 24 h (Fig. 1F). Furthermore, the blank, containing only rumen fluid, did not show remarkable changes in reducing sugars, VFAs, pH, and gas production during 48-h incubation compared with xylan treated with rumen fluid (Fig. S1).

Changes in the rumen microbial community structure

The rumen microbial community structure during the treatment of xylan with rumen fluid was analyzed by metagenomic sequencing. Good's coverage was above 99.8% in all samples, indicating sufficient sequencing

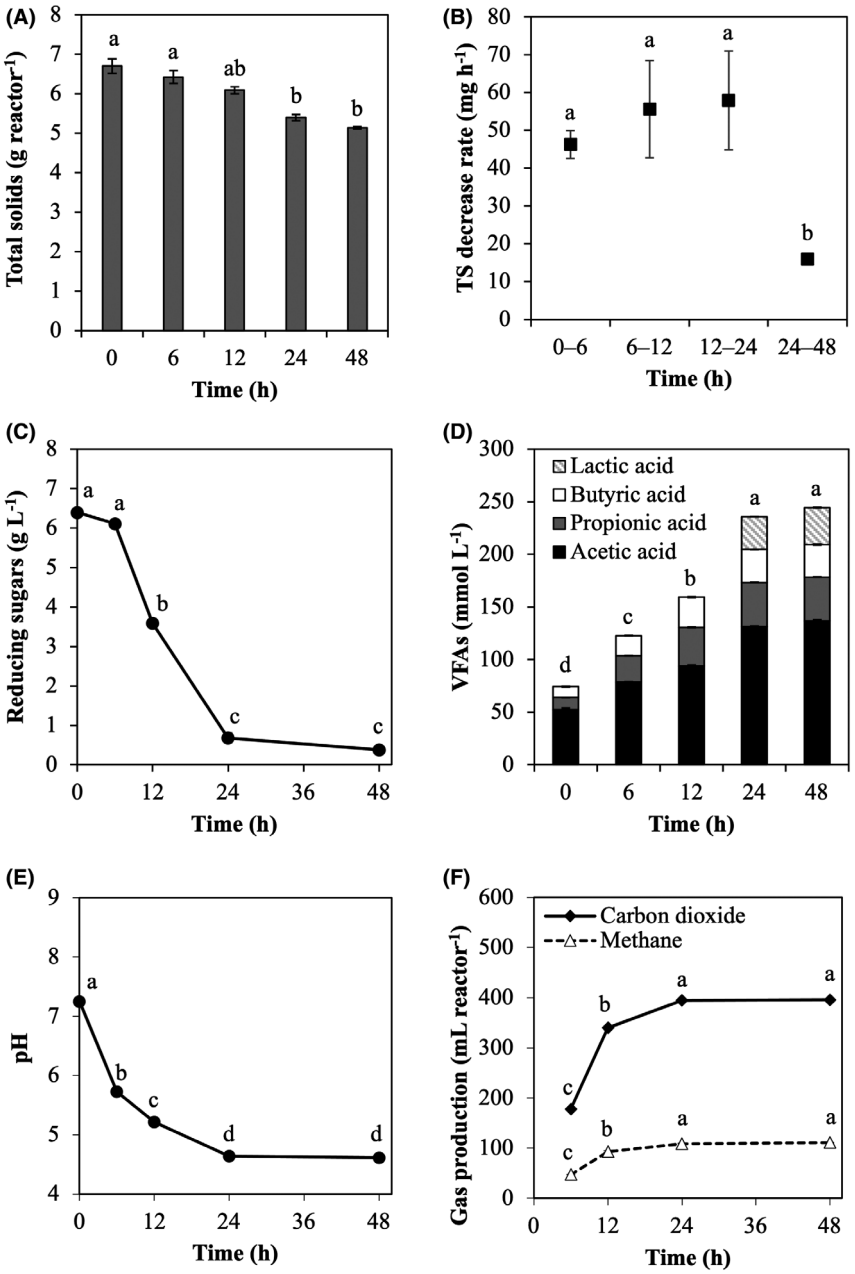

Fig. 1. Chemical characteristics of xylan degradation during treatment with the rumen fluid.
A. Total solids (TS) content.
B. TS degradation rate.
C. Reducing sugars.
D. VFAs.
E. pH.
F. Carbon dioxide and methane gas production. Multiple comparisons were conducted using the Tukey–Kramer method. Different letters indicate a statistically significant difference ($P < 0.05$).

depth (Table S1). The numbers of observed phyla and classes did not change throughout the treatment process; however, the numbers of observed orders, families, and genera were decreased at 48 h. Chao1 and ACE did not change significantly throughout the treatment process ($P > 0.05$). The diversity indices (Shannon and Simpson indices) declined during the first 6 h, increased at 12 h, and then declined after 24 h. Principal coordinate analysis indicated that the rumen microbial community structure shifted throughout the treatment process (Fig. 2A), especially from 6 h to 12 h and from 12 h to 24 h.

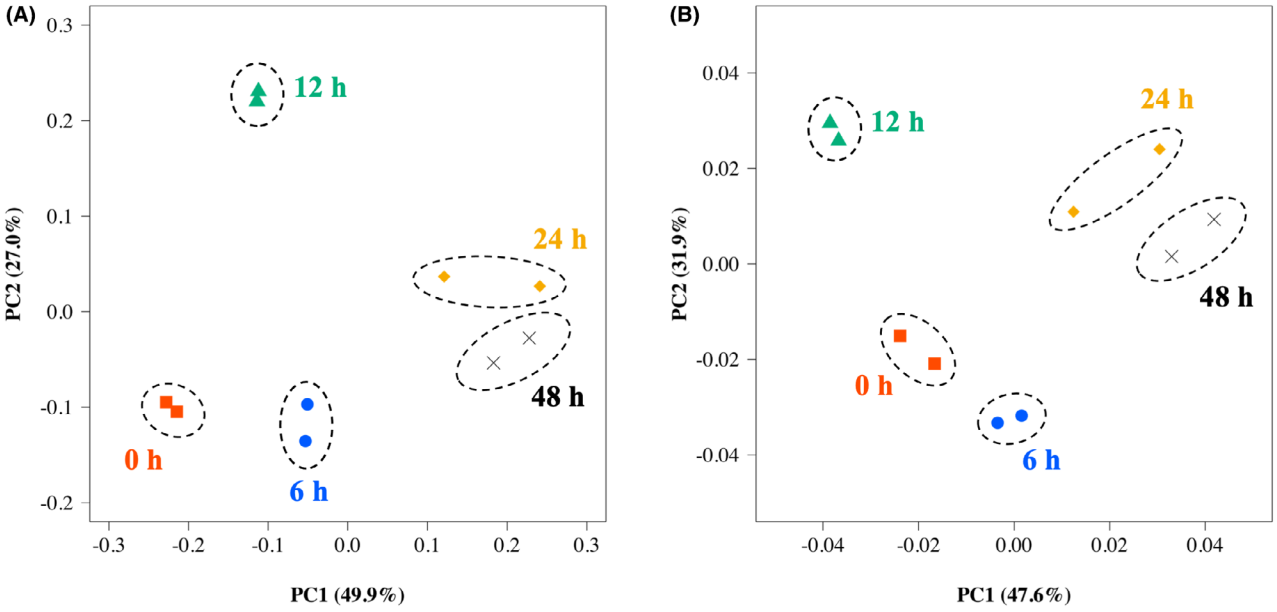

Fig. 2. Principal coordinate analysis of genus-level microbial communities (A) and COG involved in carbohydrate transport and metabolism (B) based on Bray–Curtis dissimilarities. Values in parentheses represent the amount of variation explained by each coordinate.

To investigate the shift in the rumen microbial community during xylan treatment with the rumen fluid, the taxonomic compositions of domain-, phylum-, and genus-level communities were compared (Table 1 and Fig. S2). Bacteria were the most dominant domains throughout the treatment process, and their relative abundance increased from 64.84% to 94.56% (Fig. S2A). At the phylum-level microbial community, a total of 42 phyla were identified, of which *Firmicutes* and *Bacteroidetes* were the most dominant phyla throughout the treatment process (Fig. S2B). The relative abundance of *Bacteroidetes* increased from 35.62% to 56.67% during the first 6 h, and that of *Firmicutes* increased from 20.62% to 48.84% between 6 h and 12 h. The relative abundance of unclassified *Eukaryota* decreased from 27.74% to 0.47% throughout the treatment process. At the genus-level microbial community, 544 genera were identified, 428 of which were classified as bacteria. The bacterial genus *Prevotella* was the most dominant, followed by the bacterial genera *Selenomonas*, *Lactobacillus*, *Bacteroides*, *Clostridium*, *Ruminococcus*, and *Butyrivibrio* (Table 1). The relative abundance of *Prevotella* increased by 16.72% (from 26.05% to 42.76%) during the first 6 h. The relative abundances of *Selenomonas* and *Lactobacillus* increased at 12 h and 48 h respectively. *Entodinium*, *Diploplastron*, and *Polyplastron* were the dominant protozoal genera in the rumen microbial community, and their relative abundances at 0 h were 13.67%, 4.92%, and 4.11% respectively. However, the relative abundances of all protozoal genera significantly decreased to < 1.00% after 24 h. *Neocallimastix*, *Orpinomyces*, and *Olpidium* were the dominant fungal genera in the rumen microbial community; however, their relative abundances were substantially lower than those of the dominant bacterial and protozoal genera. The relative abundances of these fungal genera decreased to 0.00% during the treatment process.

Functional characteristics of the rumen microbial community

Metagenomic sequencing revealed the functional characteristics of the rumen microbial community during xylan treatment (Figs 3 and S3). Level-1 Clusters of Orthology Groups (COG) involved in metabolism was 38.561% of total COG at 0 h and did not significantly shift during the treatment (Fig. 3A). Level-2 COG, which is involved in carbohydrate metabolism, significantly decreased by 1.565% (from 26.607% to 25.042%) between 12 h and 48 h (Fig. 3B). Principal coordinate analysis of functional COG revealed that the microbial metabolic function shifted from 6 h to 12 h and from 12 h to 24 h (Fig. 2B). Functional COG involved in beta-galactosidase/beta-glucuronidase (EC: 3.2.1.25) was the most abundant COG (6.406% of total functional COG involved in carbohydrate metabolism), followed by beta-glucosidase-related glycosidases (EC: 3.2.1.52), nucleoside-diphosphate-sugar epimerases (EC: 1.1.1.388), glycosidases (EC: 3.2.1), and phosphoenolpyruvate synthase/pyruvate phosphate dikinase (EC: 2.7.9.2) (Fig. 3). Functional COG annotated as beta-1,4-xylanase (EC: 3.2.1.8) significantly decreased by 0.268% (from 0.656% to 0.388% of total functional COG involved in

Table 1. Genus-level microbial community during treatment of xylan with the rumen fluid.

	Relative abundance (% of total abundances at each time point)				
	0 h	6 h	12 h	24 h	48 h
Bacteria					
Prevotella	26.05 ± 3.05^{cd}	42.76 ± 0.74^{a}	18.66 ± 0.48^{d}	30.12 ± 0.54^{bc}	35.57 ± 1.86^{ab}
Selenomonas	0.83 ± 0.05^{c}	1.25 ± 0.02^{c}	13.15 ± 0.42^{a}	10.24 ± 0.54^{a}	6.94 ± 1.06^{b}
Lactobacillus	0.52 ± 0.01^{b}	0.51 ± 0.02^{b}	0.34 ± 0.05^{b}	8.27 ± 3.89^{ab}	17.12 ± 2.30^{a}
Bacteroides	3.11 ± 1.05^{a}	3.50 ± 0.49^{a}	2.40 ± 0.61^{a}	4.14 ± 1.33^{a}	5.05 ± 1.20^{a}
Clostridium	3.83 ± 0.12^{ab}	3.73 ± 0.25^{b}	5.61 ± 0.61^{a}	1.56 ± 0.18^{c}	1.55 ± 0.18^{c}
Ruminococcus	3.99 ± 0.10^{a}	2.49 ± 0.10^{ab}	3.10 ± 0.32^{ab}	1.30 ± 0.52^{b}	3.10 ± 0.40^{ab}
Butyrivibrio	1.65 ± 0.01^{b}	1.90 ± 0.16^{b}	7.16 ± 0.35^{a}	1.19 ± 0.20^{bc}	0.48 ± 0.02^{c}
Parabacteroides	1.43 ± 0.06^{ab}	3.34 ± 0.53^{a}	1.72 ± 0.45^{ab}	2.08 ± 0.25^{ab}	1.37 ± 0.15^{b}
Porphyromonas	1.36 ± 0.16^{b}	1.75 ± 0.29^{ab}	1.64 ± 0.27^{ab}	2.76 ± 0.12^{a}	1.70 ± 0.24^{ab}
Bifidobacterium	0.02 ± 0.01^{b}	0.01 ± 0.01^{b}	0.13 ± 0.08^{b}	3.90 ± 1.02^{a}	1.84 ± 0.25^{ab}
Eubacterium	1.33 ± 0.02^{b}	1.08 ± 0.01^{b}	1.73 ± 0.04^{a}	0.68 ± 0.11^{c}	0.53 ± 0.05^{c}
Atopobium	0.21 ± 0.01^{a}	0.29 ± 0.06^{a}	0.66 ± 0.08^{a}	3.08 ± 1.16^{a}	0.33 ± 0.06^{a}
Barnesiella	0.48 ± 0.01^{a}	1.03 ± 0.01^{a}	0.70 ± 0.00^{a}	0.68 ± 0.17^{a}	0.82 ± 0.15^{a}
Rikenella	0.44 ± 0.09^{b}	0.65 ± 0.17^{b}	0.64 ± 0.00^{b}	1.33 ± 0.01^{a}	0.64 ± 0.08^{b}
Pseudobutyrivibrio	0.11 ± 0.01^{b}	0.35 ± 0.08^{b}	3.03 ± 0.74^{a}	0.08 ± 0.01^{b}	0.05 ± 0.02^{b}
Symbiobacterium	0.70 ± 0.13^{ab}	0.65 ± 0.05^{b}	1.33 ± 0.06^{a}	0.31 ± 0.06^{b}	0.55 ± 0.21^{b}
Bacillus	0.69 ± 0.12^{ab}	0.66 ± 0.11^{ab}	1.18 ± 0.04^{a}	0.46 ± 0.20^{b}	0.34 ± 0.07^{b}
Alistipes	0.38 ± 0.02^{b}	0.53 ± 0.04^{b}	0.39 ± 0.07^{b}	0.86 ± 0.03^{a}	0.44 ± 0.03^{b}
Desulfotomaculum	0.52 ± 0.00^{a}	0.49 ± 0.01^{a}	0.59 ± 0.02^{a}	0.31 ± 0.03^{b}	0.64 ± 0.05^{a}
Capnocytophaga	0.38 ± 0.02^{a}	0.45 ± 0.09^{a}	0.50 ± 0.04^{a}	0.65 ± 0.15^{a}	0.54 ± 0.01^{a}
Protozoa					
Entodinium	13.67 ± 2.12^{a}	4.25 ± 0.69^{b}	1.16 ± 0.06^{b}	0.91 ± 0.72^{b}	0.21 ± 0.02^{b}
Diploplastron	4.92 ± 2.13^{a}	2.30 ± 1.68^{a}	0.19 ± 0.10^{a}	0.13 ± 0.06^{a}	0.01 ± 0.00^{a}
Polyplastron	4.11 ± 0.90^{a}	0.92 ± 0.31^{b}	0.83 ± 0.03^{b}	0.10 ± 0.05^{b}	0.02 ± 0.01^{b}
Isotricha	1.08 ± 0.37^{a}	0.83 ± 0.06^{a}	3.13 ± 2.23^{a}	0.09 ± 0.06^{a}	0.07 ± 0.02^{a}
Metadinium	2.41 ± 1.40^{a}	0.08 ± 0.00^{a}	0.24 ± 0.06^{a}	0.09 ± 0.08^{a}	0.02 ± 0.02^{a}
Eudiplodinium	0.61 ± 0.11^{a}	0.74 ± 0.57^{a}	0.70 ± 0.55^{a}	0.18 ± 0.17^{a}	0.12 ± 0.00^{a}
Ophryoscolex	0.49 ± 0.48^{a}	0.00 ± 0.00^{a}	0.00 ± 0.00^{a}	0.00 ± 0.00^{a}	0.00 ± 0.00^{a}
Dasytricha	0.17 ± 0.02^{a}	0.13 ± 0.03^{a}	0.16 ± 0.07^{a}	0.00 ± 0.00^{a}	0.00 ± 0.00^{a}
Epidinium	0.01 ± 0.00^{a}	0.25 ± 0.25^{a}	0.00 ± 0.00^{a}	0.00 ± 0.00^{a}	0.00 ± 0.00^{a}
Didinium	0.07 ± 0.01^{a}	0.01 ± 0.01^{b}	0.00 ± 0.00^{b}	0.00 ± 0.00^{b}	0.00 ± 0.00^{b}
Fungi					
Neocallimastix	0.26 ± 0.00^{a}	0.09 ± 0.00^{b}	0.04 ± 0.00^{c}	0.01 ± 0.00^{d}	0.00 ± 0.00^{d}
Orpinomyces	0.11 ± 0.05^{a}	0.04 ± 0.01^{a}	0.05 ± 0.04^{a}	0.00 ± 0.00^{a}	0.00 ± 0.00^{a}
Olpidium	0.06 ± 0.00^{a}	0.02 ± 0.01^{ab}	0.00 ± 0.00^{b}	0.01 ± 0.01^{b}	0.00 ± 0.00^{b}

Top 20 bacterial genera, top 10 protozoal genera, and top 3 fungal genera are shown. All data represent the mean ± standard error. Multiple comparisons were performed using the Tukey–Kramer method, and different letters indicate a statistically significant difference ($P < 0.05$).

carbohydrate metabolism) during the first 24 h (Fig. 4A). Additionally, functional COG annotated as predicted xylanase slightly increased by 0.032% (from 0.420% to 0.452%) during the first 12 h, and then decreased to 0.360% after 24 h (Fig. 4B). Functional COG annotated as beta-xylosidase (EC: 3.2.1.37) significantly increased by 0.496% (from 1.963% to 2.459%) during the first 6 h, and then decreased to 0.16% at 12 h (Fig. 4C). Similar shifts in functional COG associated with xylan degradation were observed in the relative abundance to total abundance of functional COG. Functional COG annotated as beta-1,4-xylanase (EC: 3.2.1.8) significantly decreased by 0.027% (from 0.067% to 0.040% of total COG) during the first 24 h. Moreover, functional COG annotated as predicted xylanase increased by 0.009% (from 0.043% to 0.052% of total COG) during the first 12 h. Functional COG annotated as beta-xylosidase (EC: 3.2.1.37) significantly increased by 0.086% (from 0.200% to 0.286% of total COG) during the first 6 h.

Xylanase activity during xylan treatment

Shifts in xylanase activity during xylan treatment with rumen fluid were determined by zymography (Fig. 5). During xylan treatment with rumen fluid, the zymogram revealed a wide range of xylanases (20–250 kDa) and similar banding patterns during the first 12 h. All xylanase activities were markedly decreased at 24 h and were hardly detected at 48 h. The total peak density significantly decreased by 89.8% and 98.3% at 24 h and 48 h respectively (0 h, 70 115; 24 h, 7177; 48 h, 1166) (Fig. S6). The bands corresponding to 24, 34, 85, 180, and 200 kDa exhibited the highest peak densities throughout the treatment process and represented approximately 70% of the total peak density. Initially, the

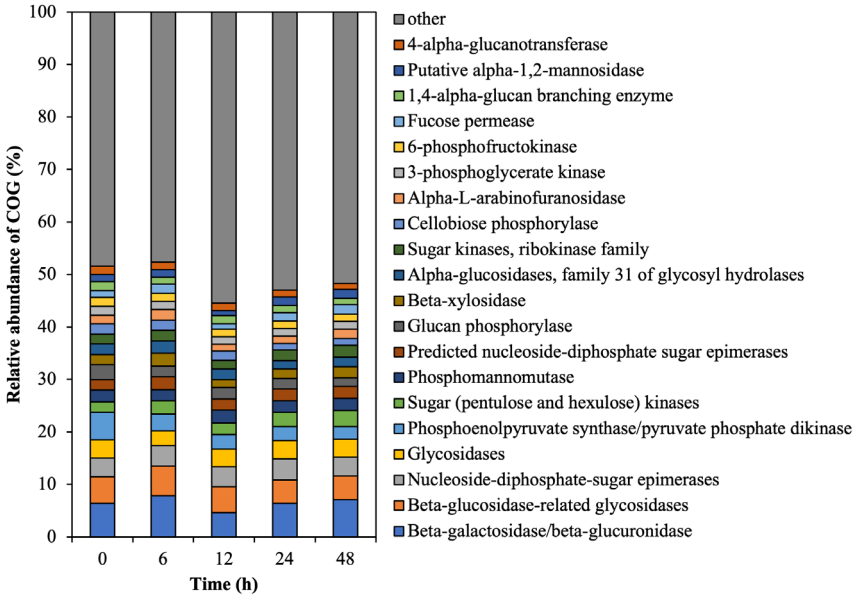

Fig. 3. Shifts in functional COG involved in carbohydrate transport and metabolism during xylan treatment with the rumen fluid. Top 20 COG are shown, and other COG are included in the category "other." All values represent the mean of two reactors.

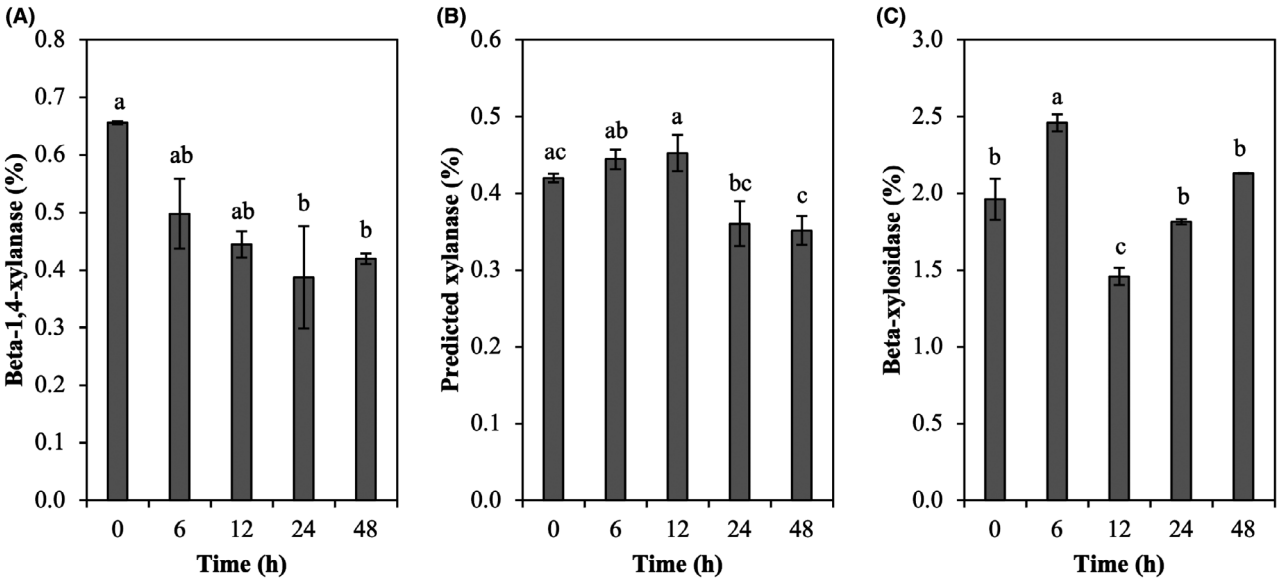

Fig. 4. Change in functional COG related to xylan degradation during treatment with the rumen fluid.
A. Beta-1,4-xylanase (EC: 3.2.1.8).
B. Predicted xylanase.
C. Beta-xylosidase (EC: 3.2.1.37). Multiple comparisons were performed using the Tukey–Kramer method, and different letters indicate a statistically significant difference ($P < 0.05$).

band at 85 kDa had the highest density, whereas the band at 180 kDa showed the highest peak density at 12 h. Shifts in peak density during the treatment process differed among the 24-, 34-, 85-, 180-, and 200-kDa bands. The band strength at 24, 34, and 85 kDa decreased throughout the treatment process, especially from 12 h to 24 h. Furthermore, the band at 180 kDa increased in density during the first 12 h, whereas it was not detected after 24 h. Similarly, the band at 200 kDa increased in density during the first 6 h and then decreased. Shifts in protein expression showed a wide range of proteins from 28 kDa to 140 kDa (Fig. S5A). The obvious bands at 85 kDa corresponding to xylanase with the highest peak density were observed during the

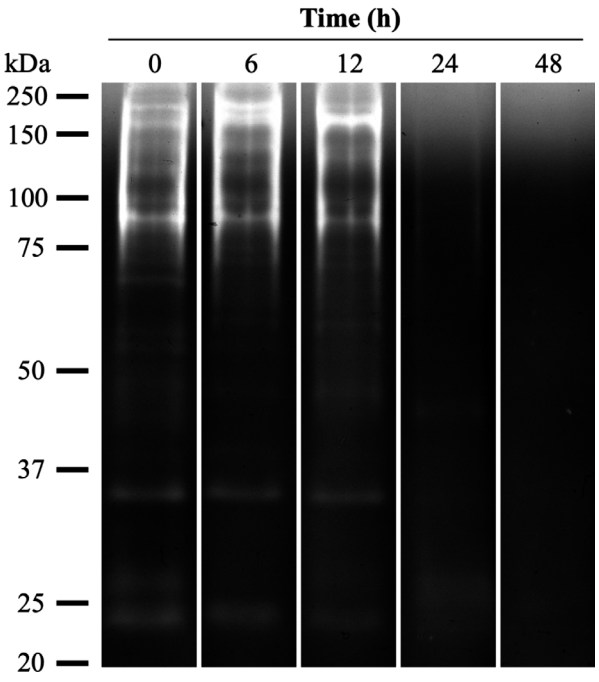

Fig. 5. Xylanase activity of rumen microbial community during xylan degradation. The pH during zymography of xylan treatment at 0, 6, 12, 24, and 48 h was 7.3, 5.7, 5.2, 4.6, and 4.6 respectively (see Fig. 1). Twenty microliters of protein extract were loaded on an 8% polyacrylamide gel containing 1.0% (*w/v*) xylan from beechwood, and incubations for xylanase zymography were performed at 37°C for 6 h. Gel images were cropped from different parts of the same gel.

first 12 h; however, its strength markedly decreased after 24 h. Other bands corresponding to the xylanases were not detected throughout the treatment of xylan.

In the blank (containing only the rumen fluid), xylanases widely ranging from 20 kDa to 250 kDa were observed, and the band patterns remained similar during the first 12 h (Fig. S4). The strength of each band decreased during the incubation. Accordingly, the total band strength decreased throughout the incubation, especially between 12 h and 24 h. The protein expression showed the bands widely ranging from 29 kDa to 68 kDa at 0 h; however, the bands were not obvious after 12 h (Fig. S5B). The bands corresponding to the xylanase with high activity were not detected.

Correlation of xylanase activity with the rumen microbial community

To predict which microorganisms contributed to the xylanase activity, the correlations between xylanase band densities and the relative abundances of ruminal microorganisms were analyzed (Fig. 6). The predominant xylanolytic bacteria, including *Prevotella*, *Clostridium*, *Ruminococcus*, and *Butyrivibrio*, did not exhibit positive correlations with xylanase activities ($P > 0.10$). Other xylanolytic genera, including *Selenomonas*, *Lactobacillus*, and *Bacteroides*, were not positively, but negatively correlated with xylanase activities ($r < -0.7$, $P < 0.05$). Besides, the protozoal genera of entodiniomorph and holotrich ciliates exhibited positive correlations with xylanase activities, except for *Metadinium* and *Ophryoscolex*. The entodiniomorph genera *Entodinium*, *Polyplastron*, and *Didinium* showed positive correlations with xylanase activity at 24 kDa ($r > 0.90$, $P < 0.05$). *Diplodinium* had a positive correlation with xylanase activities at 24 kDa ($r = 0.98$, $P < 0.01$) and 85 kDa ($r = 0.89$, $P = 0.05$). *Eudiplodinium* exhibited positive correlations with total ($r = 0.95$, $P = 0.01$), 34-kDa ($r = 0.94$, $P = 0.02$), and 180-kDa ($r = 0.88$, $P = 0.05$) xylanase activities. *Epidinium* showed a positive correlation with xylanase activity at 200 kDa ($r = 0.94$, $P = 0.02$). The holotrich genus *Isotricha* showed a positive correlation with xylanase activity at 180 kDa ($r = 0.91$, $P = 0.03$). *Dasytricha* had positive correlations with total ($r = 0.99$, $P < 0.01$), 34-kDa ($r = 0.98$, $P < 0.01$), and 85-kDa ($r = 0.93$, $P = 0.02$) xylanase activities. The predominant fungal genera *Necocallimastix*, *Orpinomyces*, and *Olpidium* had positive correlations with xylanase activities. *Neocallimastix* and *Orpinomyces* showed positive correlations with 24-kDa and 85-kDa xylanase activities ($r > 0.89$, $P < 0.05$), and *Olpidium* exhibited a positive correlation with xylanase activity at 24 kDa ($r = 0.95$, $P = 0.01$). In addition, several unclassified bacteria showed positive correlations with xylanase activities (Fig. S7). Unclassified, class *Deltaproteobacteria* exhibited positive correlations with total ($r = 0.97$, $P = 0.01$), 34-kDa ($r = 0.96$, $P = 0.01$), and 85-kDa ($r = 0.91$, $P = 0.03$) xylanase activity. Unclassified, class *Epsilonproteobacteria* and family *Bacillaceae* had a positive correlation with xylanase activity at 200 kDa ($r > 0.93$, $P < 0.05$). Unclassified, class *Clostridiales* exhibited positive correlations with total xylanase activity ($r = 0.92$, $P = 0.03$) and xylanase activities at 34 kDa ($r = 0.91$, $P = 0.03$) and 180 kDa ($r = 0.91$, $P = 0.03$). Unclassified, class *Deltaproteobacteria* showed positive correlations with total xylanase activity ($r = 0.97$, $P = 0.01$) and xylanase activities at 34 kDa ($r = 0.96$, $P = 0.01$) and 85 kDa ($r = 0.91$, $P = 0.03$). Unclassified, family *Methylococcaceae* exhibited positive correlations with total xylanase activity ($r = 0.91$, $P = 0.03$) and xylanase activities at 24 kDa ($r = 0.98$, $P < 0.01$), 34 kDa ($r = 0.93$, $P = 0.02$), and 85 kDa ($r = 0.99$, $P < 0.01$). Unclassified, families *Pasteurellaceae* and *Verrucomicrobiaceae* showed a positive correlation with xylanase activity at 24 kDa ($r > 0.88$, $P < 0.05$).

Discussion

This study revealed that a bovine rumen microbial community degraded xylan into reducing sugars, VFAs, carbon dioxide gas, and methane gas during the first 24 h of treatment, after which xylan degradation was markedly

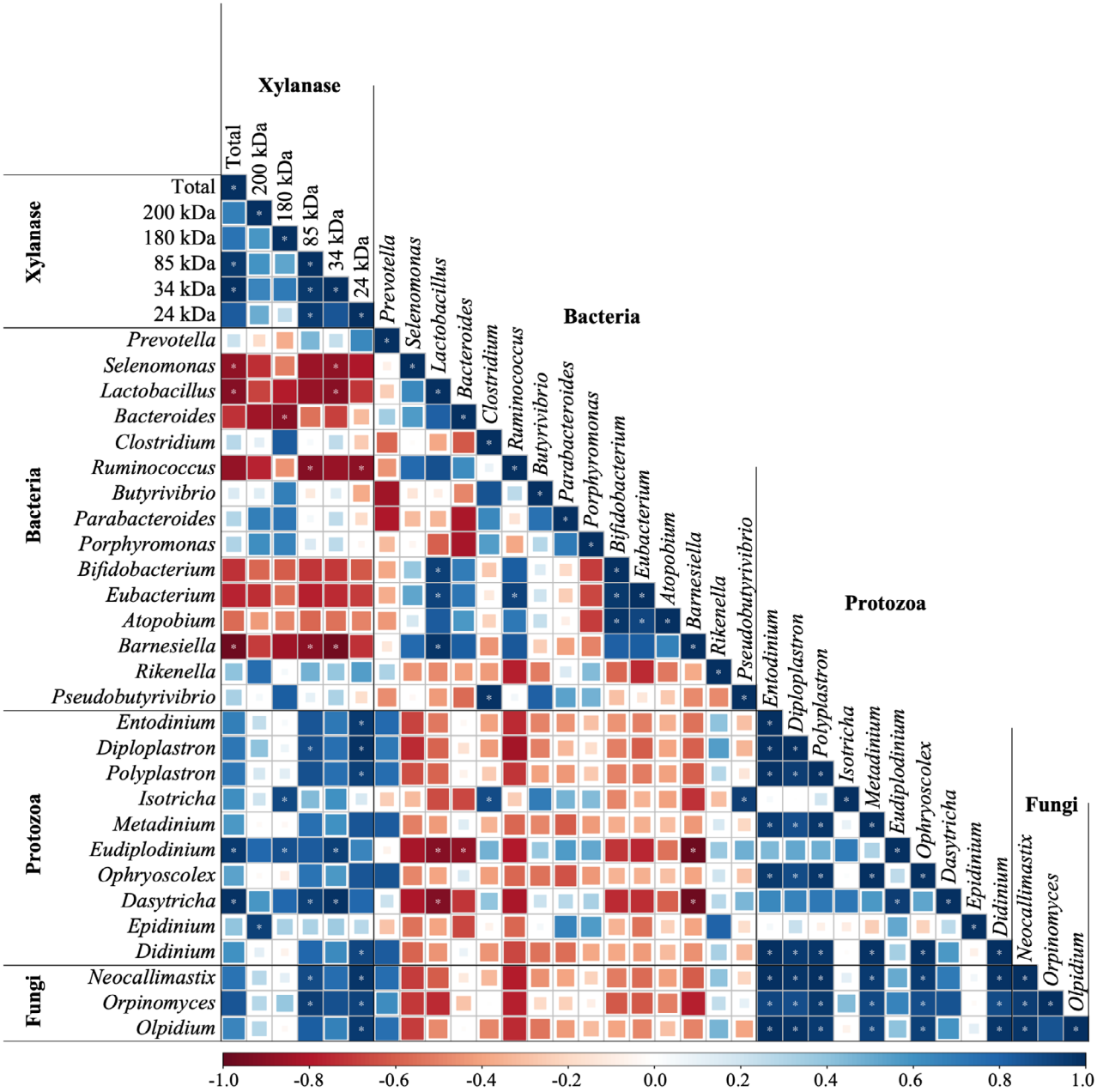

Fig. 6. Correlations of xylanase activities with relative abundances of ruminal microorganisms. Square color and size represent the correlation coefficient; blue shading represents a positive correlation, red shading represents a negative correlation, and a larger square represents a stronger correlation, whereas a smaller square represents a weaker correlation. $*P < 0.05$. Top 15 bacterial genera, top 10 protozoal genera, and top 3 fungal genera are shown.

inhibited. Zhang *et al.* (2016) treated rice straw with rumen fluid for 72 h and found four degradation phases: an initial exponential phase (0–24 h), a limiting-step phase (24–48 h), a second exponential growth phase (48–72 h), followed by a stationary phase (72–120 h) (Zhang *et al.*, 2016), which are consistent with ours. Our results also showed that the pH decreased from 7.3 to 4.6 during the first 24 h, and xylanase activities of rumen microorganisms markedly decreased after 24 h. Similarly, the alpha diversity of rumen microbial community decreased significantly after 24 h. In a previous investigation of subacute ruminal acidosis, it was reported that the bacterial alpha-diversity was lowered when ruminal pH decreased after cattle transitioned from a high-forage to a high-grain diet (Kim *et al.*, 2018). Primary fibrolytic bacteria such as xylan-degrading bacteria are intolerant

to the low ruminal pH, and rumen fiber digestion rapidly decreases when the pH drops below 6.0–6.3 (Dijkstra *et al*., 2012). We assumed that the several genera of rumen microorganisms could not survive and their numbers decreased after 48 h because of the lowered pH, which decreased the alpha diversity of rumen microbial community. In addition, lactic acid production rates increased when the pH drops to 5.0, as lactic acid-producing rumen bacteria are tolerant of low pH compared with other bacteria (Erfle *et al*., 1982). Therefore, we infer that the decrease in pH during the first 24 h inhibited the xylanolytic microorganisms, but not the VFA-producing microorganisms, resulting in a marked decline in xylan degradation and VFA accumulation after 24 h. These findings suggest that retaining a neutral pH enables xylanolytic microorganisms to degrade xylan throughout the treatment process and yields more efficient xylan biodegradation.

Metagenomic analysis showed that the structure of the rumen microbial community and functional COG shifted throughout the treatment of xylan with rumen fluid, indicating that the microbial community temporally shifted during the xylan biodegradation process. The bacterial phyla *Firmicutes* and *Bacteroidetes* were the most dominant and accounted for > 50% of the total abundance throughout treatment. Consistent herewith, our previous study reported that *Bacteroidetes* and *Firmicutes* were the dominant phyla during the treatment of rapeseed with rumen fluid for 24 h (Baba *et al*., 2017). In the genus-level bacterial community, the fibrolytic genera *Prevotella*, *Bacteroides*, *Clostridium*, and *Ruminococcus* were the dominant genera at 0 h. Dai *et al*. (2015) found that hemicellulase reads in the rumen of Holstein dairy cows fed a corn straw-containing diet were mainly derived from *Prevotella*, *Bacteroides*, *Fibrobacter*, and *Clostridium* (Dai *et al*., 2015). Their findings corroborate that the fibrolytic bacterial genera detected in this study play an important role in feed digestion in the rumen fluid collected from Holstein dairy cows. The relative abundances of *Selenomonas*, *Butyrivibrio*, and *Pseudobutyrivibrio* increased during the first 12 h. In a previous study, 13 out of 20 *Selenomonas ruminantium* isolates possessed xylanase activity, while the activities differed among the isolates (Sawanon *et al*., 2011). Genomic analysis of *Butyrivibrio* and *Pseudobutyrivibrio* revealed that these genera encoded carbohydrate-active enzymes associated with xylan degradation and suggested that the members of *Butyrivibrio* are the predominant xylan degraders (Palevich *et al*., 2020). Therefore, we infer that *Selenomonas*, *Butyrivibrio*, and *Pseudobutyrivibrio* degraded and utilized xylan for growth, which increased the relative abundances of these xylanolytic genera during the first 12 h. The relative abundances of *Lactobacillus*, *Bifidobacterium*, and *Atopobium* increased after 24 h. Several *Lactobacillus* species produce beta-D-xylosidase, which hydrolyzes xylooligosaccharides to xylose (Lasrado and Gudipati, 2013; Pontonio *et al*., 2016) and produces lactic acid from xylose (Okada *et al*., 1979). Several *Bifidobacterium* species utilize xylose, xylobiose, xylotriose, and xylooligosaccharide mixtures mainly composed of xylobiose (Okazaki *et al*., 1990), and *Bifidobacterium bifidum* produces lactic acid from xylose (de Vries and Stouthamer, 1968). *Atopobium parvulum* strain IPP 1126^{T} weakly ferments xylose and produces acid (Copeland *et al*., 2009). Thus, we speculate that *Lactobacillus*, *Bifidobacterium*, and *Atopobium* utilized xylan metabolites (i.e., xylooligosaccharides and xylose) and produced VFAs, especially lactic acid, after 24 h. The relative abundances of protozoal and fungal genera decreased during treatment. We previously reported that the relative abundances of protozoal and fungal genera significantly decreased during the treatment of carboxymethyl cellulose with rumen fluid for 48 h (Takizawa *et al*., 2020a,b,c), which was consistent with the present results. *Entodinium caudatum*, *Entodinium exiguum*, *Epidinium caudatum*, and *Ophryoscolex purkynjei* decrease in abundance when the pH decreases below 5.4, whereas they maintain their levels around pH 5.8 (Dehority, 2005). Although *Neocallimastix* R1 cannot grow in the presence of oxygen, it is sufficiently aerotolerant to survive in the air for a few hours (Trinci *et al*., 1988). From the present and previous studies, we speculate that the predominant ruminal protozoa and fungi were sensitive to current treatment conditions (i.e., the loss of essential substrates, accumulation of metabolites, low pH, physical shaking, and exposure to oxygen) and therefore declined during xylan treatment with rumen fluid. Taken together, the rumen microbial structure results indicate that the functions of the rumen microbial community temporally shift from xylan degradation to the utilization of xylan metabolites during treatment with rumen fluid. Functional analysis of the rumen microorganisms showed a decrease in xylanase after 24 h and an increase in beta-xylosidase from 12 h to 24 h, which supports the shifts in rumen microbial functions during treatment with rumen fluid.

The individual xylanases in complex rumen microbial ecosystems were visualized by xylanase zymography, which revealed that xylanase activities temporally shifted during the treatment process and significantly decreased after 24 h. We previously treated waste paper with rumen fluid for 48 h and reported that xylanase activity decreased after 24 h (Takizawa *et al*., 2019), consistently with the current results. In this study, metagenomic analyses showed that the rumen microbial community structure changed, and the relative abundances of xylanases and predicted xylanases declined from 12 to 24 h, indicating that the decrease in xylanolytic

Table 2. Correlation of dominant microorganisms in this study and their function.

Genus	This study	Previous study	
	Positive correlation	Reported xylanolytic function	Reference
Bacteria			
Prevotella	Not significant	Production of wide range of xylanases	Matsui *et al.* (2000)
Bacteroides	Negative	Transcription of hemicellulases	Dai *et al.* (2015)
Clostridium	Not significant	Transcription of hemicellulases	Dai *et al.* (2015)
Ruminococcus	Negative	Production of several xylanases	Saluzzi *et al.* (2001)
Selenomonas	Negative	Presence of xylanase activity	Sawanon *et al.* (2011)
Butyrivibrio	Not significant	Predominant xylan degrader	Palevich *et al.* (2020)
Pseudobutyrivibrio	Not significant	Encode of xylanases	Palevich *et al.* (2020)
Lactobacillus	Negative	Production of beta-D-xylosidase	Lasrado and Gudipati (2013), Pontonio *et al.* (2016)
Bifidobacterium	Not significant	Utilization of xylosaccharides	Okazaki *et al.* (1990)
Atopobium	Not significant	Fermantation of xylose	Copeland *et al.* (2009)
Fibrobacter	Not significant	Production of several xylanases	Béra-Maillet *et al.* (2004)
Unclassified bacteria			
Deltaproteobacteria	Total, 34, 85 kDa	Xylanolytic activity has been unclear.	–
Epsilonproteobacteria	200 kDa	Xylanolytic activity has been unclear.	–
Clostridiales	Total, 34, 180 kDa	Xylanolytic activity has been unclear.	–
Bacillaceae	200 kDa	Xylanolytic activity has been unclear.	–
Methylococcaceae	Total, 24, 34, 85 kDa	Xylanolytic activity has been unclear.	–
Pasteurellaceae	24 kDa	Xylanolytic activity has been unclear.	–
Verrucomicrobiaceae	24 kDa	Xylanolytic activity has been unclear.	–
Protozoa			
Entodinium	24 kDa	Presence of xylanase activity	Takenaka *et al.* (2004)
Diploplastron	24, 85 kDa	Presence of xylanase activity	Wereszka *et al.* (2006)
Polyplastron	24 kDa	Xylanases of 26, 32, 38, and 52 kDa	Devillard *et al.* (1999), Béra-Maillet *et al.* (2005)
Isotricha	180 kDa	No gas production from xylan	Takenaka *et al.* (2004)
Eudiplodinium	Total, 34, 180 kDa	Xylanases of 26, 42, and 54 kDa	Béra-Maillet *et al.* (2005)
Dasytricha	Total, 85, 180 kDa	Presence of xylanase activity	Takenaka *et al.* (2004)
Epidinium	200 kDa	Presence of xylanase activity	Takenaka *et al.*, 2004
Didinium	24 kDa	Xylanolytic activity has been unclear.	–
Fungi			
Neocallimastix	24, 85 kDa	Production of xylanases	Krause *et al.* (2003)
Orpinomyces	24, 85 kDa	Production of xylanases	Krause *et al.* (2003)
Olpidium	24 kDa	Xylanolytic activity has been unclear.	–

microorganisms resulted in low xylanase activity after 24 h. An assessment of protein expression revealed that the protein at 85 kDa was abundant during the first 12 h. Quantification of band densities also showed that xylanases of 24, 34, 85, 180, and 200 kDa were highly active during the period in which xylan was efficiently degraded into VFAs, carbon dioxide gas, and methane gas. Our results indicated that these xylanases, especially 85 kDa of xylanase, contributed to xylan biodegradation during treatment with rumen fluid. As mentioned above, a previous metatranscriptomic analysis revealed that two-thirds of putative hemicellulases were produced by members of the genera *Ruminococcus*, *Prevotella*, and *Fibrobacter* (Dai *et al.*, 2015). *Ruminococcus* produces xylanases of 32, 85, and 210 kDa (Saluzzi *et al.*, 2001), *Prevotella* produces a wide range of xylanases from 60–170 kDa (Matsui *et al.*, 2000), and *Fibrobacter* produces several xylanases between 35 kDa and 130 kDa (Béra-Maillet *et al.*, 2004). Therefore, we hypothesize that these three genera produce high-activity xylanases and contribute to xylan degradation during treatment with rumen fluid. The relative abundances of *Selenomonas*, *Butyrivibrio*, and *Pseudobutyrivibrio* increased during xylan degradation, which indicated that these xylanolytic genera also contributed to xylan degradation. However, correlation analyses of xylanase activities with the relative abundances of rumen microorganisms indicated that xylanolytic bacterial genera, namely, *Ruminococcus*, *Prevotella*, *Fibrobacter*, *Butyrivibrio*, *Selenomonas*, *Butyrivibrio*, and *Pseudobutyrivibrio*, did not contribute to xylanase activity (Table 2). Investigation of rumen microorganisms during *in situ* incubation of switchgrass revealed that changes in the microbiome were particularly prevailing within 30 min and after 4 h of rumen incubation (Piao *et al.*, 2014). Therefore, we infer that the xylanolytic bacterial genera produced high-activity xylanases and contributed to xylan degradation during the initial treatment phase (from 0 h to 6 h). Of note, positive correlations between xylanolytic bacterial genera and xylanase activities might have been observed in a more detailed microbial analysis. Further investigation of the temporal dynamics of xylanase activities and xylanolytic bacterial genera is needed to elucidate the contribution of bacterial genera

to xylan degradation during treatment with rumen fluid. Several genera of rumen protozoa and fungi showed significantly positive correlations with xylanase activities. The functional roles of rumen protozoa and fungi in ruminal fermentation and carbohydrate metabolism remain obscure. Rumen protozoa account for a large portion of the biomass in the rumen microbial community. *Dasytricha ruminantium*, *Epidinium caudatum*, *Polyplastron multivesiculatum*, and *Entodinium* spp. have xylanase activity (Takenaka *et al*., 2004). *Diploplastron affine* shows the xylanolytic activity and produces at least two xylanases (Wereszka *et al*., 2006). *Polyplastron multivesiculatum* produces xylanases of 26, 32, 38, and 52 kDa (Devillard *et al*., 1999; Béra-Maillet *et al*., 2005), and *Eudiplodinium maggii* produces xylanases of 26, 42, and 54 kDa (Béra-Maillet *et al*., 2005). Rumen fungal species, such as *Neocallimastix frontalis*, *Neocallimastix particiarum*, and *Orpinomyces* sp., produce endoxylanases and degrade lignified tissue that is not degraded by other microorganisms (Krause *et al*., 2003). Our results suggest that rumen protozoa and fungi contribute to xylanase activity and xylan biodegradation during treatment with rumen fluid. Interestingly, unclassified bacteria positively correlated with xylanase activities. Although the xylanolytic function of unclassified bacteria remains unknown, unclassified bacteria are considered to produce various xylanases and contribute to the degradation of lignocellulosic biomass. Metagenomic analysis revealed that a high proportion of unclassified bacteria were attached to rice straw throughout incubation in the rumen (Cheng *et al*., 2017). A metatranscriptomic analysis showed that most of the transcripts encoding putative proteins involved in the degradation of plant cell-wall polysaccharides were < 90% similar to known species at the amino acid sequence level (Dai *et al*., 2015). In this study, unclassified bacteria possibly played an important role in xylan degradation during treatment with rumen fluid. Altogether, our results suggest that rumen protozoa (*Entodinium*, *Diploplastron*, *Polyplastron*, *Isotricha*, *Eudiplodinium*, *Dasytricha*, *Epidinium*, and *Didinium*), fungi (*Neocallimastix*, *Orpinomyces*, and *Olpidium*), and unclassified bacteria (*Deltaproteobacteria*, *Epsilonproteobacteria*, *Clostridiales*, *Bacillaceae*, *Methylococcaceae*, *Pasteurellaceae*, and *Verrucomicrobiaceae*) are associated with xylanase activities of 24, 34, 85, 180, and 200 kDa, which results in xylan biodegradation into VFAs and gas during the treatment with rumen fluid.

In conclusion, the results of this study suggested the relationships among the changes in xylan degradation, xylanase activities, microbial function, and microbial structure (Fig. 7). The chemical analysis revealed that the rumen microorganisms degrade xylan into reducing sugars, VFAs, carbon dioxide gas, and methane gas

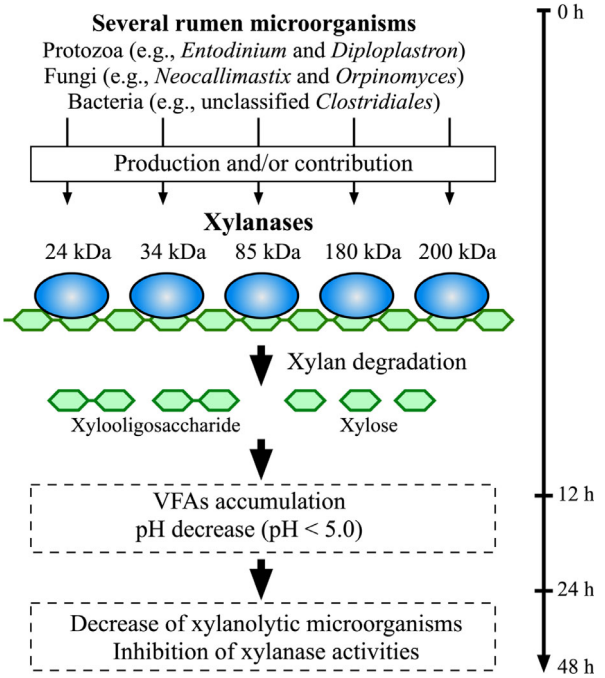

Fig. 7. Summary of xylanase degradation suggested in this study.

during the first 24 h, whereas this activity was inhibited at 48 h of xylan treatment with the rumen fluid. Zymography showed that xylanase activities temporally shifted during treatment. Xylanases were active during the first 12 h of treatment; however, their activities considerably decreased after 24 h. The metagenomic analysis indicated a decrease in functional COG annotated as xylanase and a change in the structure of microbial community during 24 h. The relative abundance of several protozoan and fungal genera, as well as unclassified bacteria, showed a positive correlation with the xylanase activities. Taken together, our study suggests that several protozoa (*Entodinium*, *Diploplastron*, *Polyplastron*, *Isotricha*, *Eudiplodinium*, *Dasytricha*, *Epidinium*, and *Didinium*), fungi (*Neocallimastix*, *Orpinomyces*, and *Olpidium*), and unclassified bacteria (*Deltaproteobacteria*, *Epsilonproteobacteria*, *Clostridiales*, *Bacillaceae*, *Methylococcaceae*, *Pasteurellaceae*, and *Verrucomicrobiaceae*) are associated with the xylanase activities and xylan degradation into sugars, VFAs, and gas during the 24 h treatment with rumen fluid. Although this study focused on the association between the relative abundance of rumen microorganisms and xylanase activities, the absolute abundance of rumen microorganisms and xylanase expression are also important for determining key xylanolytic microorganisms. To identify the key microorganisms contributing to xylan degradation, quantitative and metatranscriptomic analysis are required. Our findings suggest that supplementation and activation

of pivotal microorganisms associated with xylan degradation can effectively boost lignocellulosic biomass bioconversion into bioenergy.

Experimental procedures

Treatment of xylan with rumen fluid

All experiments were approved and performed in accordance with the regulations of the Institutional Animal Care and Use Committee of Tohoku University. A Holstein cow was fed a diet consisting of 64% timothy grass and 36% concentrate and allowed *ad libitum* access to water. The rumen fluid was collected from the Holstein cow at 2 h post-feeding, using a stomach tube. The collected rumen fluid was transferred to the laboratory within 30 min, and then filtered through a 1 × 1-mm mesh to remove coarse solids. After the filtration, the rumen fluid was immediately used for treatment of xylan.

Treatment with the rumen fluid was conducted according to our previous studies (Takizawa *et al.*, 2018, 2020a,b,c). Xylan powder obtained from corn cores (Tokyo Chemical Industry UK, Tokyo, Japan) was used as a substrate. Four grams of xylan powder were mixed with 200 ml of rumen fluid and purged with nitrogen gas to remove oxygen. Xylan treatment was conducted in a 250-ml reactor on a rotary shaker at 170 r.p.m. at 37°C for 48 h. A blank reactor containing only rumen fluid was incubated under the same conditions. All incubations were conducted in duplicate.

Chemical analysis

To evaluate xylan biodegradation rate into metabolic products, TS, reducing sugars, VFAs, and gas production were determined as described previously (Takizawa, *et al.*, 2020). Briefly, TS were measured after drying the rumen samples at 105°C overnight. Liquid samples were filtered using a cellulose acetate membrane filter (0.45 μm pore diameter). Reducing sugars were determined by the Somogyi–Nelson method (Nelson, 1944; Somogyi, 1945) using a UV-VIS spectrophotometer (Shimadzu, Kyoto, Japan). VFA concentrations were determined by high-performance liquid chromatography (Jasco, Tokyo, Japan) using an ion-exchange column (RSpak KC-811; Jasco). The pH was measured with a pH meter (LAQUAtwin; HORIBA, Tokyo, Japan). Gas concentrations (methane and carbon dioxide) were measured by gas chromatography (GC-8A; Shimadzu) with a packed column (Shincarbon-ST; Restek, Bellefonte, PA, USA). A unit equipped with a thermal conductivity detector was connected to an integrator (C-R8A; Shimadzu). Argon gas was used as the carrier gas, and the temperature of injection and detection was set to 100°C and 120°C respectively.

Sodium dodecyl sulfate-polyacrylamide gel electrophoresis (SDS-PAGE) and zymography

The rumen fluids were mixed with equal volumes of 2× radioimmunoprecipitation assay buffer (Nacalai Tesque, Kyoto, Japan) containing 2 mM of phenylmethylsulfonyl fluoride and 1× proteinase inhibitor (Sigma-Aldrich, Tokyo, Japan). Proteins were extracted using Lysing Matrix E tubes (MP Biomedicals, Solon, OH, USA). One milliliter of supernatant was mixed with 100 μl of trichloroacetic acid, incubated on ice for 30 min, and centrifuged at 17 000 *g* for 10 min. After removing the supernatant, 1 ml of acetone at −20°C was mixed with the pellet, and the suspension was centrifuged at 17 000 *g* for 10 min. This process was repeated, and the pellets were dried at room temperature. The dried pellets were solubilized in 1 ml of 2× sample buffer comprising 20% (*v*/*v*) glycerol, 4% (*w*/*v*) SDS, 0.01% (*w*/*v*) bromophenol blue, 0.125 M Tris-HCl (pH 7.4), 10% (*v*/*v*) 2-mercaptoethanol, 2 mM phenylmethylsulfonyl fluoride, and 1× proteinase inhibitor (Sigma-Aldrich). SDS-PAGE and zymography were conducted according to a previous study (Takizawa *et al.*, 2020a,b,c), with some modifications. Briefly, the supernatants were heated at 70°C for 20 min and immediately cooled on ice. Twenty microliters of protein extract were separated on an 8% polyacrylamide gel containing 1.0% (*w*/*v*) xylan from beechwood (Nacalai Tesque) at 200 V for 60 min. Separated proteins were refolded in 2.5% (*v*/*v*) Triton X-100 for 60 min. The gel was soaked in 50 mM of sodium acetate buffer (pH 6.5) for 15 min, followed by incubation in 30 mM of sodium acetate buffer at 37°C for 6 h (observed pH values during treatment were applied for zymography). After incubation, the gel was soaked in distilled water at 4°C and then in 30 mM of sodium acetate buffer (pH 6.5). The gel was stained with 0.1% (*w*/*v*) Congo Red and de-stained with 1 M NaCl to visualize endoglucanase activity. Next, the gel was soaked in 0.3% (*v*/*v*) acetic acid to enhance the intensity of active bands. Band densities were quantified using the ImageJ software (Schindelin *et al.*, 2012). In addition, SDS-PAGE was performed as mentioned earlier, and the gels were stained with 0.1% (*w*/*v*) Coomassie Brilliant Blue to investigate the protein expression during the treatment of xylan.

Metagenomic analysis

DNA extraction and metagenomic sequencing were carried out as previously described (Takizawa *et al.*, 2020a, b,c). Briefly, total DNA was extracted from 2 ml of rumen fluid using the FastDNA SPIN Kit for Soil (MP Biomedicals) according to the manufacturer's instructions. DNA libraries were constructed using the QIAseq FX DNA

Library Kit (Qiagen, Hilden, Germany) following the manufacturer's protocol. The sizes of the constructed DNA libraries were determined with an Agilent 2100 Bioanalyzer (Agilent, Santa Clara, CA, USA) using the Agilent High Sensitivity DNA Kit (Agilent). Paired-end sequencing was conducted on an Illumina HiSeq X instrument (Illumina, San Diego, CA, USA).

Paired-end sequences were uploaded to Metagenome Rapid Annotation using Subsystem Technology server version 4.0.3 (Meyer *et al*., 2008) for functional and taxonomic annotations. After quality filtering, a total of 137 048 176 sequences (average 13 704 818; minimum 9 942 341; maximum 17 581 176) were obtained from the samples. Hierarchical functional predictions were performed against the COG database (*E* value of $< 10^{-5}$, identity cut-off of $> 60\%$, and alignment length of > 30). To explore the rumen microbial community structure, rRNA sequences were identified by BLAST searching against the Silva SSU database (*E* value of $< 10^{-5}$, alignment length of > 15 bp) on Metagenome Rapid Annotation using Subsystem Technology. Sequences are available at Metagenome Rapid Annotation using Subsystem Technology under the project accession mgp88122.

Statistical analysis

Pearson's correlation coefficient and significance levels were evaluated and illustrated using the R package CORRPLOT, version 0.84 (Wei and Simko, 2017), to determine the relationships between endoglucanase band densities and relative abundances of ruminal microorganisms. Good's coverage was calculated using the R package QsRutils, version 0.1.4 (John, 2020). Alpha (chao1, ACE, Shannon, and Simpson) and beta diversity analyses involving principal coordinate analysis based on Bray–Curtis dissimilarity were conducted using the R package VEGAN, version 2.5.6 (Jari *et al*., 2019). Multiple comparisons were performed according to the Tukey–Kramer method using the R package MULTCOMP, version 1.4.13 (Hothorn *et al*., 2008), and statistical significance was declared at $P < 0.05$.

Acknowledgements

The authors highly thank Mr. Yoshimi Yokoyama, Mr. Shigetoshi Akasaka, and Ms. Takako Sasaki (Field Science Center, Graduate School of Agricultural Science, Tohoku University, Miyagi, Japan) for providing technical support during cow rumen fluid collection and chemical analysis.

Conflict of interest

The authors declare no competing interests.

References

Baba, Y., Matsuki, Y.U., Mori, Y., Suyama, Y., Tada, C., Fukuda, Y., *et al*. (2017) Pretreatment of lignocellulosic biomass by cattle rumen fluid for methane production: Bacterial flora and enzyme activity analysis. *J Biosci Bioeng* **123:** 489–496.

Baba, Y., Matsuki, Y.U., Takizawa, S., Suyama, Y., Tada, C., Fukuda, Y., *et al*. (2019) Pretreatment of lignocellulosic biomass with cattle rumen fluid for methane production: fate of added rumen microbes and indigenous microbes of methane seed sludge. *Microbes Environ* **34:** 421–428.

Baba, Y., Tada, C., Fukuda, Y., and Nakai, Y. (2013) Improvement of methane production from waste paper by pretreatment with rumen fluid. *Bioresour Technol* **128:** 94–99.

Béra-Maillet, C., Devillard, E., Cezette, M., Jouany, J.P., and Forano, E. (2005) Xylanases and carboxymethylcellulases of the rumen protozoa *Polyplastron multivesiculatum*, *Eudiplodinium maggii* and *Entodinium* sp. *FEMS Microbiol Lett* **244:** 149–156.

Béra-Maillet, C., Ribot, Y., and Forano, E. (2004) Fiber-degrading systems of different strains of the genus *Fibrobacter*. *Appl Environ Microbiol* **70:** 2172–2179.

Castillo-González, A.R., Burrola-Barraza, M.E., Domínguez-Viveros, J., and Chávez-Martínez, A. (2014) Rumen microorganisms and fermentation. *Arch Med Vet* **46:** 349–361.

Cheng, Y., Wang, Y., Li, Y., Zhang, Y., Liu, T., Wang, Y.U., *et al*. (2017) Progressive colonization of bacteria and degradation of rice straw in the rumen by Illumina sequencing. *Front Microbiol* **8:** 2165.

Comtet-Marre, S., Parisot, N., Lepercq, P., Chaucheyras-Durand, F., Mosoni, P., Peyretaillade, E., *et al*. (2017) Metatranscriptomics reveals the active bacterial and eukaryotic fibrolytic communities in the rumen of dairy cow fed a mixed diet. *Front Microbiol* **8:** 67.

Copeland, A., Sikorski, J., Lapidus, A., Nolan, M., Del Rio, T.G., Lucas, S., *et al*. (2009) Complete genome sequence of *Atopobium parvulum* type strain (IPP 1246T). *Stand Genomic Sci* **1:** 166–173.

Dahmen, N., Lewandowski, I., Zibek, S., and Weidtmann, A. (2018) Integrated lignocellulosic value chains in a growing bioeconomy: status quo and perspectives. *GCB Bioenergy* **11:** 107–117.

Dai, X., Tian, Y., Li, J., Su, X., Wang, X., Zhao, S., *et al*. (2015) Metatranscriptomic analyses of plant cell wall polysaccharide degradation by microorganisms in the cow rumen. *Appl Environ Microbiol* **81:** 1375–1386.

Dehority, B.A. (2005) Effect of pH on viability of *Entodinium caudatum*, *Entodinium exiguum*, *Epidinium caudatum*, and *Ophryoscolex purkynjei* in vitro. *J Eukaryot Microbiol* **52:** 339–342.

Devillard, E., Newbold, C.J., Scott, K.P., Forano, E., Wallace, R.J., Jouany, J.P., and Flint, H.J. (1999) A xylanase produced by the rumen anaerobic protozoan *Polyplastron multivesiculatum* shows close sequence similarity to family 11 xylanases from Gram-positive bacteria. *FEMS Microbiol Lett* **181:** 145–152.

Dijkstra, J., Ellis, J.L., Kebreab, E., Strathe, A.B., López, S., France, J., and Bannink, A. (2012) Ruminal pH regulation

and nutritional consequences of low pH. *Anim Feed Sci Technol* **172:** 22–33.

Erfle, J.D., Boila, R.J., Teather, R.M., Mahadevan, S., and Sauer, F.D. (1982) Effect of pH on fermentation characteristics and protein degradation by rumen microorganisms in vitro. *J Dairy Sci* **65:** 1457–1464.

Guo, W., Wang, W., Bi, S., Long, R., Ullah, F., Shafiq, M., *et al*. (2020) Characterization of anaerobic rumen fungal community composition in Yak, Tibetan sheep and small tail han sheep grazing on the Qinghai-Tibetan Plateau. *Animals* **10:** 144.

Hothorn, T., Bretz, F., and Westfall, P. (2008) Simultaneous inference in general parametric models. *Biometrical J* **50:** 346–363.

Jari, O., Guillaume, F.B., Michael, F., Roeland, K., Pierre, L., Dan, M., *et al*. (2019) *vegan: community ecology package*. R package version 2.5-6. R Package version 340.

John, Q. (2020) *QsRutils: R functions useful for community ecology*. R package version 0.1.4.

Kim, Y.H., Nagata, R., Ohkubo, A., Ohtani, N., Kushibiki, S., Ichijo, T., and Sato, S. (2018) Changes in ruminal and reticular pH and bacterial communities in Holstein cattle fed a high-grain diet. *BMC Vet Res* **14:** 310.

Krause, D.O., Denman, S.E., Mackie, R.I., Morrison, M., Rae, A.L., Attwood, G.T., and McSweeney, C.S. (2003) Opportunities to improve fiber degradation in the rumen: Microbiology, ecology, and genomics. *FEMS Microbiol Rev* **27:** 663–693.

Lasrado, L.D., and Gudipati, M. (2013) Purification and characterization of β-d-xylosidase from Lactobacillus brevis grown on xylo-oligosaccharides. *Carbohydr Polym* **92:** 1978–1983.

Liang, J., Nabi, M., Zhang, P., Zhang, G., Cai, Y., Wang, Q., *et al*. (2020) Promising biological conversion of lignocellulosic biomass to renewable energy with rumen microorganisms: A comprehensive review. *Renew Sustain Energy Rev* **134:** 110335.

Matsui, H., Ogata, K., Tajima, K., Nakamura, M., Nagamine, T., Aminov, R.I., and Benno, Y. (2000) Phenotypic characterization of polysaccharidases produced by four Prevotella type strains. *Curr Microbiol* **41:** 45–49.

Meyer, F., Paarmann, D., D'Souza, M., Olson, R., Glass, E.M., Kubal, M., *et al*. (2008) The metagenomics RAST server – a public resource for the automatic phylogenetic and functional analysis of metagenomes. *BMC Bioinformatics* **9:** 386.

Nelson, N. (1944) A photometric adaptation of the somogyi method for the determination of glucose. *J Biol Chem* **3:** 375–380.

Novotná, Z., Procházka, J., Šimůnek, J., and Fliegerová, K. (2010) Xylanases of anaerobic fungus *Anaeromyces mucronatus*. *Folia Microbiol (Praha)* **55:** 363–367.

Nyonyo, T., Shinkai, T., and Mitsumori, M. (2014) Improved culturability of cellulolytic rumen bacteria and phylogenetic diversity of culturable cellulolytic and xylanolytic bacteria newly isolated from the bovine rumen. *FEMS Microbiol Ecol* **88:** 528–537.

Okada, S., Kozaki, M., and Suzuki, Y. (1979) A new heterofermentative Lactobacillus species with meso-diaminopimelic acid in peptidoglycan, *Lactobacillus vaccinostercus kozaki* and *okada* sp. nov. *J Gen Appl Microbiol* **25:** 215–221.

Okazaki, M., Fujisawa, S., and Matsumoto, N. (1990) Effect of xylooligosaccharide on the growth of Bifidobacteria. *Bifidobact Microflora* **9:** 77–86.

Palevich, N., Kelly, W.J., Leahy, S.C., Denman, S., Altermann, E., Rakonjac, J., and Attwood, G.T. (2020) Comparative genomics of rumen *Butyrivibrio* spp. uncovers a continuum of polysaccharide-degrading capabilities. *Appl Environ Microbiol* **86.**

Piao, H., Lachman, M., Malfatti, S., Sczyrba, A., Knierim, B., Auer, M., *et al*. (2014) Temporal dynamics of fibrolytic and methanogenic rumen microorganisms during in situ incubation of switchgrass determined by 16s rRNA gene profiling. *Front Microbiol* 5.

Pontonio, E., Mahony, J., Di Cagno, R., O'Connell Motherway, M., Lugli, G.A., O'Callaghan, A., *et al*. (2016) Cloning, expression and characterization of a β-d-xylosidase from *Lactobacillus rossiae* DSM 15814T. *Microb Cell Fact* **15:** 72.

Saluzzi, L., Flint, H.J., and Stewart, C.S. (2001) Adaptation of *Ruminococcus flavefaciens* resulting in increased degradation of ryegrass cell walls. *FEMS Microbiol Ecol* **36:** 131–137.

Sawanon, S., Koike, S., and Kobayashi, Y. (2011) Evidence for the possible involvement of *Selenomonas ruminantium* in rumen fiber digestion. *FEMS Microbiol Lett* **325:** 170–179.

Sawatdeenarunat, C., Surendra, K.C., Takara, D., Oechsner, H., and Khanal, S.K. (2015) Anaerobic digestion of lignocellulosic biomass: challenges and opportunities. *Bioresour Technol* **178:** 178–186.

Schindelin, J., Arganda-Carreras, I., Frise, E., Kaynig, V., Longair, M., Pietzsch, T., *et al*. (2012) Fiji: an open-source platform for biological-image analysis. *Nat Methods* **9:** 676–682.

Somogyi, M. (1945) Determination of blood sugar. *J Biol Chem* **160:** 69–74.

Takenaka, A., Tajima, K., Mitsumori, M., and Kajikawa, H. (2004) Fiber digestion by rumen ciliate protozoa. *Microbes Environ* **19:** 203–210.

Takizawa, S., Abe, K., Fukuda, Y., Feng, M., Baba, Y., Tada, C., and Nakai, Y. (2020a) Recovery of the fibrolytic microorganisms from rumen fluid by flocculation for simultaneous treatment of lignocellulosic biomass and volatile fatty acid production. *J Clean Prod* **257:** 120626.

Takizawa, S., Asano, R., Fukuda, Y., Feng, M., Baba, Y., Abe, K., *et al*. (2020b) Change of endoglucanase activity and rumen microbial community during biodegradation of cellulose using rumen microbiota. *Front Microbiol* **11:** 1–12.

Takizawa, S., Baba, Y., Tada, C., Fukuda, Y., and Nakai, Y. (2020c) Sodium dodecyl sulfate improves the treatment of waste paper with rumen fluid at lower concentration but decreases at higher condition. *J Mater Cycles Waste Manag* **22:** 656–663.

Takizawa, S., Baba, Y., Tada, C., Fukuda, Y., and Nakai, Y. (2018) Pretreatment with rumen fluid improves methane production in the anaerobic digestion of paper sludge. *Waste Manag* **78:** 379–384.

Takizawa, S., Baba, Y., Tada, C., Fukuda, Y., and Nakai, Y. (2019) Preservation of rumen fluid for the pretreatment of waste paper to improve methane production. *Waste Manag* **87:** 672–678.

Trinci, A.P.J., Lowe, S.E., Milne, A., and Theodorou, M.K. (1988) Growth and survival of rumen fungi. *BioSystems* **21:** 357–363.

de Vries, W., and Stouthamer, A.H. (1968) Fermentation of glucose, lactose, galactose, mannitol, and xylose by bifidobacteria. *J Bacteriol* **96:** 472–478.

Wang, L., Zhang, G., Xu, H., Xin, H., and Zhang, Y. (2019) Metagenomic analyses of microbial and carbohydrate-active enzymes in the rumen of holstein cows fed different forage-to-concentrate ratios. *Front Microbiol* **10:** 649.

Wei, T., and Simko, V. (2017) *R package "corrplot": visualization of a correlation matrix*. R package version 0.84.

Wereszka, K., Michałowski, T., Newbold, C., and McEwan, N. (2006) Xylanolytic activity of the rumen protozoan *Diploplastron affine*. *J Anim Feed Sci* **15:** 43–46.

Zhang, H., Zhang, P., Ye, J., Wu, Y., Fang, W., Gou, X., and Zeng, G. (2016) Improvement of methane production from rice straw with rumen fluid pretreatment: A feasibility study. *Int Biodeterior Biodegrad* **113:** 9–16.

Supporting information

Additional supporting information may be found online in the Supporting Information section at the end of the article.

Fig. S1. Changes in chemical characteristics of the rumen fluid in a blank (containing only the rumen fluid). (A) Reducing sugars; (B) VFAs; (C) pH; and (D) carbon dioxide and methane gas production. Multiple comparisons were conducted using the Tukey–Kramer method, and different letters indicate a statistically significant difference ($P < 0.05$).

Fig. S2. Taxonomic composition of the domain-level (A) and phylum-level (B) community. The relative abundances of predominant phyla were shown. All abundances represent the mean of two reactors.

Fig. S3. Changes in the structure of level-1 COG (A), level-2 COG involved in metabolism (B) during the treatment of xylan with the rumen fluid. All values represent the mean of two reactors.

Fig. S4. Xylanase activity in the blank.The pH during zymography of xylan treatment was 7.0 (see Fig. S1). Twenty microliters of protein extract were loaded on an 8% polyacrylamide gel containing 1.0% (*w/v*) xylan from beechwood, and incubations for xylanase zymograms were conducted at 37°C for 6 h. Gel images were cropped from different parts of the same gel.

Fig. S5. SDS-PAGE of proteins extracted from rumen microbial community in the treatment of xylan (A) and the blank containing only the rumen fluid (B). Twenty microliters of the protein extract were loaded on 8% polyacrylamide gel and stained with 0.1% Coomassie Brilliant Blue solution.

Fig. S6. Total and five xylanases activities that had a high peak density during the treatment of xylan with the rumen fluid.

Fig. S7. Correlations of xylanase activities with relative abundances of unclassified microorganisms.Square color and size represent each correlation coefficient; blue shading represents a positive correlation, red shading represents a negative correlation, and a larger square represents a stronger correlation, whereas a smaller square represents a weaker correlation. $*P < 0.05$.

Table S1. Alpha diversity during the treatment of xylan with the rumen fluid. All data represent the mean $\pm$ standard error. Multiple comparisons were conducted using the Tukey–Kramer method, and different letters indicate a statistically significant difference ($P < 0.05$).

